

# A Novel Sensitive Turn-on Fluorescent $Zn^{2+}$ Chemosensor Based on an Easy To Prepare $C_3$ -Symmetric Schiff-Base Derivative in 100% Aqueous Solution

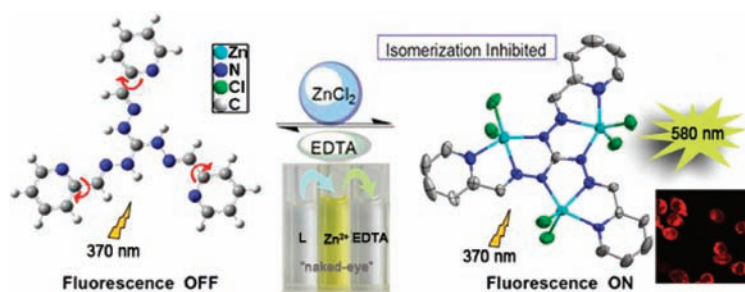
Ying Zhou,<sup>†</sup> Zhan-Xian Li,<sup>†</sup> Shuang-Quan Zang,<sup>\*,†</sup> Yan-Yan Zhu,<sup>†</sup> Hong-Yan Zhang,<sup>\*,‡</sup> Hong-Wei Hou,<sup>†</sup> and Thomas C. W. Mak<sup>†,§</sup>

The College of Chemistry and Molecular Engineering, Zhengzhou University, Zhengzhou 450001, People's Republic of China, Key Laboratory of Photochemical Conversion and Optoelectronic Materials, Technical Institute of Physics and Chemistry, Chinese Academy of Sciences, Beijing, People's Republic of China, and Department of Chemistry and Center of Novel Functional Molecules, The Chinese University of Hong Kong, Shatin, New Territories, Hong Kong SAR, People's Republic of China

zangsqzg@zzu.edu.cn; zhanghongyan@mail.ipc.ac.cn

Received December 24, 2011

## ABSTRACT



A  $C_3$ -symmetric Schiff-base example of the new simple, low cost, highly water soluble, and sensitive turn-on fluorescent  $Zn^{2+}$  chemosensor is described. The sensor was successfully applied to the detection of intracellular  $Zn^{2+}$ . Moreover, the sensor could also serve as a potential recyclable component in sensing materials. Notably, the color change is so obvious that all of the recycling process can be seen clearly by the naked eye.

A chemosensor is the type of compound that renders a significant change in magnetic, electronic, electrical, or optical properties when it binds to a specific guest molecule

or ion. Among various types of sensors, fluorescent chemosensors for metal ions have attracted much attention due to their convenient use and high sensitivity, and they have been employed to clarify the real-time dynamics and various biological functions of targeted metal cations in living cells.<sup>1</sup> The zinc ion, as the second most abundant and essential trace element in the human body behind iron, plays a significant role in various fundamental biological processes, such as cellular metabolism, gene expression, apoptosis, neurotransmission, regulation of metalloenzymes,

<sup>†</sup> Zhengzhou University.

<sup>‡</sup> Technical Institute of Physics and Chemistry, Chinese Academy of Sciences.

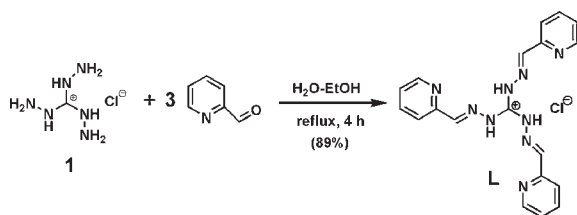
<sup>§</sup> The Chinese University of Hong Kong.

(1) (a) Meng, Q.-T.; Zhang, X.-L.; He, C.; He, G.-J.; Zhou, P.; Duan, C.-Y. *Adv. Funct. Mater.* **2010**, *20*, 1903. (b) Ishida, M.; Naruta, Y.; Tani, F. *Angew. Chem., Int. Ed.* **2010**, *49*, 91. (c) He, G.-J.; Zhang, X.-L.; He, C.; Zhao, X.-W.; Duan, C.-Y. *Tetrahedron* **2010**, *66*, 9762. (d) Jung, H. S.; Kwon, P. S.; Lee, J. W.; Kim, J. I.; Hong, C. S.; Kim, J. W.; Yan, S.; Lee, J. Y.; Lee, J. H.; Joo, T.; Kim, J. S. *J. Am. Chem. Soc.* **2009**, *131*, 2008. (e) Suresh, M.; Shrivastav, A.; Mishra, S.; Suresh, E.; Das, A. *Org. Lett.* **2008**, *10*, 3013. (f) Suresh, M.; Ghosh, A.; Das, A. *Chem. Commun.* **2008**, 3906. (g) Numata, M.; Li, C.; Bae, A.-H.; Kaneko, K.; Sakurai, K.; Shinkai, S. *Chem. Commun.* **2005**, 4655.

(2) (a) Zhou, X.-Y.; Yu, B.-R.; Guo, Y.-L.; Tang, X.-L.; Zhang, H.-H.; Liu, W.-S. *Inorg. Chem.* **2010**, *49*, 4002. (b) Qian, F.; Zhang, C.-L.; Zhang, Y.-M.; He, W.-J.; Gao, X.; Hu, P.; Guo, Z.-J. *J. Am. Chem. Soc.* **2009**, *131*, 1460. (c) Berg, J. M.; Shi, Y. *Science* **1996**, *271*, 1081. (d) Vallee, B. L.; Falchuk, K. H. *Physiol. Rev.* **1993**, *73*, 79.

and DNA binding or recognition.<sup>2</sup> Thus far, a number of fluorescence-enhancement-based chemosensors for Zn(II)-selective detection were reported and have been used with some success in biological applications.<sup>3</sup> Nevertheless, most of the reported fluorescent as well as colorimetric sensors for Zn<sup>2+</sup> function in either pure organic or organic–aqueous solutions. This limits their practical applications in a physiological environment. Moreover, their preparations require laborious multistep organic synthesis, which renders their discovery processes slow and causes prohibitively high cost. In this context, the design and synthesis of simple, facile, and efficient Zn<sup>2+</sup> probes remains of great interest,<sup>2a</sup> particularly for those with high solubility in a solely water system and selectivity and photostability in the spectral visible region.

### Scheme 1. Synthesis of Fluorescent Sensor L



To our knowledge, C<sub>3</sub>-symmetric ligands can be regarded as triangular building blocks. This type of ligand can adopt different conformations and bind in a number of coordination modes, according to the geometric requirements of the metal ions, and may offer avenues for the construction of organometallic frameworks with a variety of structures.<sup>4</sup> Herein, we report a new fluorescent chemosensor, tris(2-pyridinecarboxaldehyde)triaminoguanidinium chloride (**L**), which is the first C<sub>3</sub>-symmetric Schiff-base example that shows an excellent solubility in 100% aqueous media with a highly sensitive fluorescence turn-on property upon binding to Zn<sup>2+</sup>. More importantly, compound **L** can be readily prepared by a simple and low-cost Schiff-base reaction of picolinaldehyde with triaminoguanidinium chloride (Scheme 1; details are available in the Supporting Information).

The organic framework of **L** possesses an approximate planar structure with three equivalent cavities capable of chelating Zn<sup>2+</sup> ions. The formation of a Zn(II) complex can enhance the coplanarity of the conjugated system, leading to a rather rigid structure with quite strong fluorescence

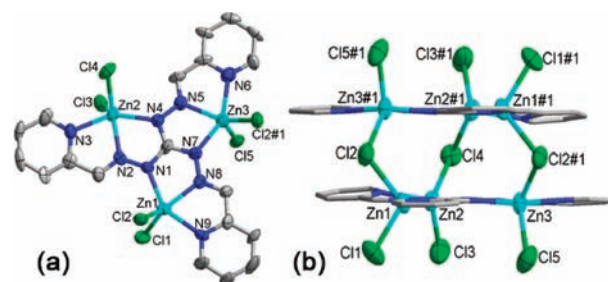


**Figure 1.** X-ray crystal structure of the zinc complex of **L**: (a) trinuclear unit and (b) side view of the hexanuclear Zn(II) complex. All hydrogen atoms and solvent molecules were omitted for clarity. Symmetry code: (#1)  $-x + 1, y, -z + 0.5$ .

properties, as compared to those of the free compound **L**. Figure 1 shows the single-crystal X-ray structure of the hexanuclear Zn(II) complex (**L**-Zn<sup>2+</sup>), which confirms the formation of the quite stable drumlike structure of this complex. The solid-state structure of the **L**-Zn<sup>2+</sup> complex consists of two planar trinuclear units bridged by three chlorine atoms. We have investigated the sensor's chemodosimetric properties, which can provide a sensitive measurement of Zn<sup>2+</sup> in an absolute aqueous environment. Furthermore, for presenting its application in biological samples, the application of **L** to cultured A549 lung adenocarcinoma cells was implemented and discussed.

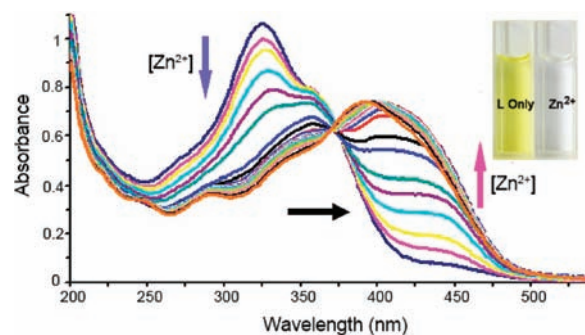


**Figure 2.** UV–vis spectra of **L** (50 μM) upon the titration of Zn<sup>2+</sup> (0.2, 0.4, 0.6, 0.8, 1.0, 1.2, 1.4, 1.6, 1.8, 2.0, 2.5, and 3.0 equiv) in buffer solution (10 mM Tris–HCl, pH 7.54) with an excitation of 370 nm.

(3) (a) Peng, X.; Wu, T.; Fan, J.; Wang, J.; Zhang, S.; Song, F.; Sun, S. *Angew. Chem., Int. Ed.* **2011**, *50*, 4180. (b) Xu, Z.; Yoon, J.; Spring, D. R. *Chem. Soc. Rev.* **2010**, *39*, 1996. (c) Guo, Z.-Q.; Zhu, W.-H.; Zhu, M.-M.; Wu, X.-M.; Tian, H. *Chem. Eur. J.* **2010**, *16*, 14424. (d) Liu, Z.-P.; Zhang, C.-L.; Li, Y.-L.; Wu, Z.-Y.; Qian, F.; Yang, X.-L.; He, W.-J.; Gao, X.; Guo, Z.-J. *Org. Lett.* **2009**, *11*, 795. (e) Felton, C. E.; Harding, L. P.; Jones, J. E.; Kariuki, B. M.; Pope, S. J. A.; Rice, C. R. *Chem. Commun.* **2008**, 6185. (f) Wang, H.-H.; Gan, Q.; Wang, X.-J.; Xue, L.; Liu, S.-H.; Jiang, H. *Org. Lett.* **2007**, *9*, 4995.

(4) (a) Hu, X.-Y.; Wang, J.; Zhu, X.; Dong, D.-P.; Zhang, X.-L.; Wu, S.-O.; Duan, C.-Y. *Chem. Commun.* **2011**, 11507. (b) Zeng, X.; Dong, L.; Wu, C.; Mu, L.; Xue, S.-F.; Tao, Z. *Sens. Actuators B: Chem.* **2009**, *141*, 506. (c) Hu, X. L.; Rodriguez, I. C.; Meyer, K. *J. Am. Chem. Soc.* **2004**, *126*, 13464. (d) Bretonnière, Y.; Mazzanti, M.; Wietzke, R.; Pécaut, J. *Chem. Commun.* **2000**, 1543.

indicates the formation of only one UV-active zinc complex. Meanwhile, two new absorption peaks appeared at 245 and 288 nm with some changes in pattern, and a maximum absorbance at 396 nm was observed when the  $\text{Zn}^{2+}$  concentration was increased to 3 equiv. Subsequently, the absorption spectrum remained at a plateau upon further addition of  $\text{Zn}^{2+}$  ( $> 3$  equiv). These observations imply the undoubted conversion of free compound **L** to the corresponding zinc complex.

Figure 3 shows the change of fluorescence spectra of **L** upon addition of  $\text{Zn}^{2+}$ . Compound **L** alone displayed a weak, single fluorescence emission band at 483 nm with a negligible fluorescence quantum yield ( $< 0.002$ ) when it was excited at 370 nm. A  $\text{Zn}^{2+}$  titration experiment led to a prominent fluorescence enhancement, accompanied by a perceived color change from colorless to dark yellow, indicating a  $\text{Zn}^{2+}$ -selective OFF–ON fluorescent signaling behavior. The increased in emission intensity may be attributed to the formation of the **L**- $\text{Zn}^{2+}$  complex, in which the  $\text{C}=\text{N}$  isomerization<sup>5</sup> and proton transfer (ESPT)<sup>6</sup> are inhibited. Meanwhile, upon binding  $\text{Zn}^{2+}$ , **L** exhibited a large emission bathochromic shift of 97 nm from 483 to 580 nm, indicating that chemosensor **L** recognizes  $\text{Zn}^{2+}$  partially based on the chelation-enhanced fluorescence (CHEF) mechanism.<sup>7</sup> In comparison to that of free **L** in aqueous buffer a  $\sim 21$ -fold significant fluorescence enhancement could be observed when 3.0 equiv of  $\text{Zn}^{2+}$  was present. Both the Job plot and Bensi–Hildebrand analysis were implemented, demonstrating a 1/3 stoichiometry for the **L**- $\text{Zn}^{2+}$  complexation, which is in good agreement with results from single-crystal X-ray structural analysis (Figures S6 and S7, Supporting Information). The association constants of **L** with Zn were calculated as  $K_{\text{Zn1}} = 1.9 \times 10^5$ ,  $K_{\text{Zn2}} = 1.5 \times 10^4$ , and  $K_{\text{Zn3}} = 6.1 \times 10^3$ , respectively, by literature methods.<sup>8</sup> The fluorescent titration profile of **L** with  $\text{Zn}^{2+}$  (Figure S8) demonstrated that the detection limit of  $\text{Zn}^{2+}$  is  $2.5 \times 10^{-6}$  M under the experimental conditions used here. After  $\text{Zn}^{2+}$  was added into a buffer solution of **L**, the fluorescence decay curve was fitted to double-exponential decay (Figure S9).

Achieving a higher selectivity toward a specific analyte over other potentially competing species is a necessity for a fluorescence chemosensor.<sup>3c</sup> We evaluated the emission response of **L** against different transition-metal ions in buffer solutions and found that only  $\text{Zn}^{2+}$  caused a significant ratio signal output (Figure 4). Although the addition of  $\text{Cd}^{2+}$  also

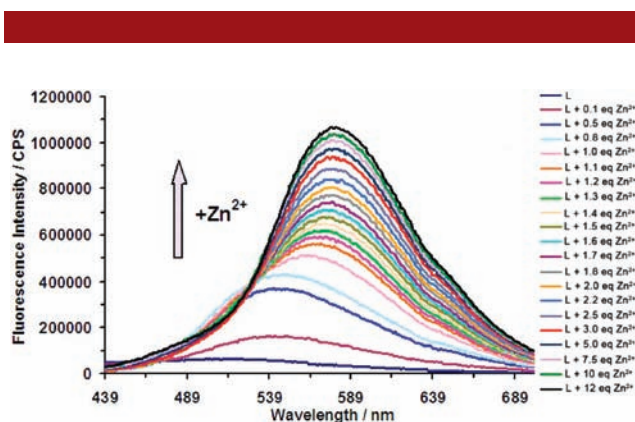


**Figure 3.** Emission spectra of **L** ( $5 \times 10^{-5}$  M) obtained in Tris–HCl buffer (10 mM, pH 7.54) when titrated with  $\text{Zn}^{2+}$  ( $\lambda_{\text{ex}}$  370 nm). The final ratio of  $\text{Zn}^{2+}$  ion to **L** is 12 equiv.

induced an emission enhancement to a certain extent, this enhancement was less pronounced as compared to that of  $\text{Zn}^{2+}$ . Also, it should be noted that addition of  $\text{Cd}^{2+}$  induced a red shift of emission from 483 to 532 nm, which is quite different from that of  $\text{Zn}^{2+}$ . Fortunately,  $\text{Cd}^{2+}$  as a highly toxic heavy-metal ion in vivo has a very low concentration. This small interference does not affect the probe's application in physiological detection. As is well-known, the physiologically important metal ions  $\text{Na}^+$ ,  $\text{K}^+$ ,  $\text{Mg}^{2+}$ , and  $\text{Ca}^{2+}$  exist at high concentration in living cells. In our case, they were measured at a concentration as high as 1 mM. As expected, these cations exerted a negligible effect on the fluorescence response for **L**. Similar phenomena were also observed with the addition of  $\text{Hg}^{2+}$ ,  $\text{Cr}^{3+}$ ,  $\text{Fe}^{3+}$ ,  $\text{Pb}^{2+}$ ,  $\text{Ni}^{2+}$ , and  $\text{Co}^{2+}$ , respectively. Only  $\text{Cu}^{2+}$  might form a complex with **L** and obviously quenched the fluorescence.<sup>9</sup>

The selectivity of **L** for  $\text{Zn}^{2+}$  over other transition-metal ions has been examined. Results of our studies have revealed that all potentially competitive metal cations (except  $\text{Cu}^{2+}$ ) exerted no or little influence on the fluorescence detection of  $\text{Zn}^{2+}$  in aqueous buffer solutions. In order to understand the strong quenching behavior of  $\text{Cu}^{2+}$ , we have measured the change in emission intensity of **L**- $\text{Zn}^{2+}$  with increasing  $\text{Cu}^{2+}$  ion concentrations (Figure S10). The emission intensity of **L**- $\text{Zn}^{2+}$  at  $\sim 580$  nm showed a gradual decrease, indicating that  $\text{Cu}^{2+}$  can displace  $\text{Zn}^{2+}$  to form a **L**- $\text{Cu}^{2+}$  complex. In this regard, the complex **L**- $\text{Zn}^{2+}$  can be considered as a good ON–OFF chemosensor candidate for  $\text{Cu}^{2+}$ . In addition, the effects of counterions on the selective properties of  $\text{Zn}^{2+}$  demonstrated that  $\text{Zn}^{2+}$  salts such as  $\text{Zn}(\text{NO}_3)_2$ ,  $\text{Zn}(\text{ClO}_4)_2$ ,  $\text{ZnBr}_2$ ,  $\text{Zn}(\text{SO}_4)_2$ , and  $\text{Zn}(\text{CH}_3\text{COO})_2$  showed almost similar spectral changes of **L**- $\text{ZnCl}_2$  (Figures S11 and S12), which suggests that the counteranion effects are negligibly small.

In order to obtain a better understanding of the interactions between **L** and  $\text{Zn}^{2+}$ , we studied the chemical reversibility of

(5) (a) Wu, J.-S.; Liu, W.-M.; Ge, J.-C.; Zhang, H.-Y.; Wang, P.-F. *Chem. Soc. Rev.* **2011**, *40*, 3483. (b) Suresh, M.; Mandal, A. K.; Saha, S.; Suresh, E.; Mandoli, A.; Liddo, R. D.; Parnigotto, P. P.; Das, A. *Org. Lett.* **2010**, *12*, 5406. (c) Ray, D.; Bharadwaj, P. K. *Inorg. Chem.* **2008**, *47*, 2252. (d) Sheng, J.-R.; Feng, F.; Qiang, Y.; Liang, F.-G.; Sen, L.; Wei, F.-H. *Anal. Lett.* **2008**, *41*, 2203.

(6) (a) Zhang, X.; Guo, L.; Wu, F.-Y.; Jiang, Y.-B. *Org. Lett.* **2003**, *5*, 2667. (b) Sengupta, P. K.; Kasha, M. *Chem. Phys. Lett.* **1979**, *68*, 382.

(7) (a) Ma, T.-H.; Dong, M.; Dong, Y.-M.; Wang, Y.-W.; Peng, Y. *Chem. Eur. J.* **2010**, *16*, 10313. (b) Xue, L.; Liu, Q.; Jiang, H. *Org. Lett.* **2009**, *11*, 3454. (c) Jiang, P.-J.; Guo, Z.-J. *Coord. Chem. Rev.* **2004**, *248*, 205. (d) Akkaya, E. U.; Huston, M. E.; Czarnik, A. W. *J. Am. Chem. Soc.* **1990**, *112*, 3590.

(8) (a) Zhao, Q.; Li, R.-F.; Xing, S.-K.; Liu, X.-M.; Hu, T.-L.; Bu, X.-H. *Inorg. Chem.* **2011**, *50*, 10041. (b) Valeur, B. *Molecular Fluorescence: Principles and Applications*; Wiley-VCH: Weinheim, Germany, 2001.

(9) (a) Li, Z.-X.; Yu, M.-M.; Zhang, L.-F.; Yu, M.; Liu, J.-X.; Wei, L.-H.; Zhang, H.-Y. *Chem. Commun.* **2010**, *46*, 7169. (b) Peng, X.-J.; Du, J.-J.; Fan, J.-L.; Wang, J.-Y.; Wu, Y.-K.; Zhao, J.-Z.; Sun, S.-G.; Xu, T. *J. Am. Chem. Soc.* **2007**, *129*, 1500. (c) Zheng, Y.; Orbulescu, J.; Ji, X.; Andreopoulos, F. M.; Pham, S. M.; Leblanc, R. M. *J. Am. Chem. Soc.* **2003**, *125*, 2680.



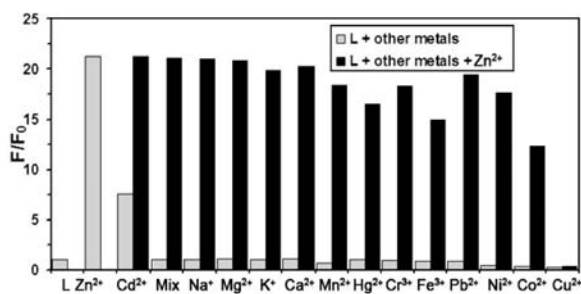


**Figure 4.** Fluorescence responses of **L** to various metal ions (gray bars) and fluorescence change of the mixture of **L** and  $\text{Zn}^{2+}$  after addition of an excess of the appropriate metal ions (black bars). The equiv ratio of **L** to each of  $\text{Ca}^{2+}$ ,  $\text{Mg}^{2+}$ ,  $\text{Na}^+$ ,  $\text{K}^+$  is 1/20, and the equiv ratio of **L** to each of the other transition-metal ions is 4. Mix:  $\text{Zn}^{2+} + \text{Na}^+/\text{K}^+/\text{Mg}^{2+}/\text{Ca}^{2+}$ ,  $\lambda_{\text{ex}}$  370 nm.

the binding of **L** to  $\text{Zn}^{2+}$  in buffer solutions. As seen by the naked eye, the yellow color of a solution of **L-Zn**<sup>2+</sup> gradually disappeared upon the addition of excess disodium EDTA (Figures S13 and S14). The effects of pH on the fluorescence of the free compound **L** and its complex **L-Zn**<sup>2+</sup> are shown in Figures S15 and S16, respectively. Over the pH range we tested, compound **L** alone was not sensitive to pH. However, the fluorescence intensity of **L-Zn**<sup>2+</sup> displayed a strong pH dependence, as illustrated by its fluorescence intensity at 580 nm. The resulting sigmoidal curve (Figure S15) gives a  $\text{p}K_{\text{a}}$  value of 6.5. An intense and stable fluorescence of **L-Zn**<sup>2+</sup> in the pH range 7.0–10.0 warrants its application in monitoring intracellular  $\text{Zn}^{2+}$  without being affected by changes in physiological pH values.

The ability of biosensing molecules to selectively monitor guest species in living systems is of great importance for biological applications.<sup>1d</sup> We have measured the sensitivity of **L** to  $\text{Zn}^{2+}$  in human lung adenocarcinoma epithelial cells (A549) by using laser scanning confocal microscopy (Nikon C1Si). Fluorescence images were recorded with a Spinhole aperture, 100% gain of detector, and an oil objective with 60 $\times$  magnification and 1.40 NA. After A549 cells were incubated with **L** ( $10^{-2}$   $\mu\text{mol}$ ) and PBS (1 mL) for 1 h at 37  $^{\circ}\text{C}$ , no obvious fluorescence could be imaged (Figure 5a). However, when the cells were supplemented with exogenous  $\text{ZnCl}_2$  ( $3 \times 10^{-2}$   $\mu\text{mol}$ ) in the growth medium for 10 min at 37  $^{\circ}\text{C}$ , washed with 1 mL of PBS, and then loaded with **L** and incubated for another 1 h under the same experimental conditions, a significant fluorescence increase from the intracellular region was clearly observed, although the zinc complex has a relatively lower quantum yield ( $\Phi_{\text{f}} = 0.01$ ) (Figure 5b). The strong fluorescence resulted from the reaction of **L** and intracellular  $\text{Zn}^{2+}$  ions. The bright field transmission image of these A549 cells in Figure 5c is exactly the same as the fluorescence image in Figure 5b, confirming an intracellular fluorescence image.

To gain an additional understanding of the mechanism of the fluorescence behavior of **L** and its chelation complex

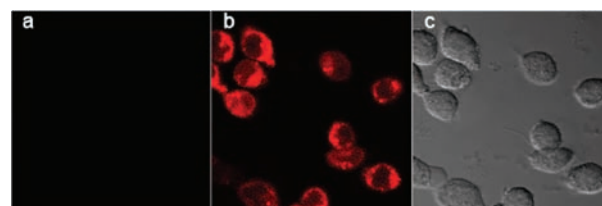


**Figure 5.** Imaging of intracellular  $\text{Zn}^{2+}$  in A549 cells at 37  $^{\circ}\text{C}$  with use of confocal microscopy: (a) cells incubated with **L** ( $10^{-2}$   $\mu\text{mol}$ ) for 1 h; (b) cells incubated with  $\text{ZnCl}_2$  ( $3 \times 10^{-2}$   $\mu\text{mol}$ ) aqueous solution for 10 min and washed with PBS, then incubated for another 1 h after being treated with **L** ( $10^{-2}$   $\mu\text{mol}$ ); (c) bright field image of A549 cells in parts a and b. Emission was collected at a 600/75 nm detector channel upon excitation at 408 nm by a diode laser.

**L-Zn**<sup>2+</sup>, density functional theory (DFT) and time-dependent DFT (TDDFT) calculations were carried out. The optimized structures and the contribution of each electronic oscillator (orbital transition) to the lowest energy transition are all shown in the Supporting Information (Figures S17 and S18, Table S1). The calculated dihedral angles of **L-Zn**<sup>2+</sup> are in good agreement with the experimental crystal structure (Table S2). From the results of these calculations, the introduction of  $\text{Zn}^{2+}$  onto the group can distinctly affect the steric hindrance and electronic structure of the imine when  $\text{C}=\text{N}$  isomerization takes place. Such localization of the electronic densities and increase of the structural rigidity of the sensor **L** upon  $\text{Zn}^{2+}$  complexation could be attributable to both the emission enhancement and red shift.

In conclusion, we have presented a simple, water-soluble, and  $\text{C}_3$ -symmetric Schiff-base example of a highly selective fluorescent chemosensor for  $\text{Zn}^{2+}$ . The complex features a large  $\text{Zn}^{2+}$ -induced red emission shift (97 nm) and a distinguishable color change from colorless to dark yellow under complete aqueous physiological conditions when  $\text{Zn}^{2+}$  was present. Notably, the chemically reversible binding of **L** to  $\text{Zn}^{2+}$  showed **L** could serve as a potential recyclable component in sensing materials. In addition, the complex **L-Zn**<sup>2+</sup> could be considered as a good ON–OFF  $\text{Cu}^{2+}$  sensor candidate. Specifically, the new probe's water solubility and membrane permeability are favorable for its potential application in intracellular imaging of  $\text{Zn}^{2+}$ .

**Acknowledgment.** We gratefully acknowledge financial support by the National Natural Science Foundation of China (No. 20901070) and Zhengzhou University (No. 000001307106).

**Supporting Information Available.** Text, figures, tables, and a CIF file giving experimental procedures, characterization data, including supplementary spectral data,  $^1\text{H}/^{13}\text{C}$  NMR and mass spectra, and crystallographic data for **L-Zn**<sup>2+</sup>. This material is available free of charge via the Internet at <http://pubs.acs.org>.

The authors declare no competing financial interest.